

Eur. Phys. J. C  
DOI 10.1146/epjc.12012.299.42214

THE EUROPEAN  
PHYSICAL JOURNAL C

Regular Article - Experimental Physics

## First proton–proton collisions at the LHC as observed with the ALICE detector: measurement of the charged-particle pseudorapidity density at $\sqrt{s} = 900$ GeV

The ALICE Collaboration

K. Aamodt<sup>27</sup>, N. Abiel<sup>17</sup>, U. Akech<sup>28</sup>, A. Aleksa<sup>29</sup>, S. Alkhalaf<sup>30</sup>, A. Alvarez Quintero<sup>31</sup>, A. Aloisio<sup>32</sup>, D. Adamo<sup>33</sup>, M.M. Aggarwal<sup>34</sup>, G. Aglieri Rinella<sup>35</sup>, A.G. Aghajani<sup>36</sup>, S. Aguilera Salazar<sup>37</sup>, Z. Akhmedov<sup>38</sup>, A. Ahmad<sup>39</sup>, N. Ahmad<sup>40</sup>, S.H. Ahn<sup>41</sup>, R. Akhmetov<sup>42</sup>, A. Akindroev<sup>43</sup>, D. Aleksandrov<sup>44</sup>, R. Alessandrino<sup>45</sup>, R. Alfaro Molina<sup>46</sup>, A. Alici<sup>47</sup>, K. Almaraz Vega<sup>48</sup>, J. Alme<sup>49</sup>, T. Alt<sup>50</sup>, V. Altin<sup>51</sup>, S. Altinpinar<sup>52</sup>, C. Andrei<sup>53</sup>, A. Andronic<sup>54</sup>, G. Anelli<sup>55</sup>, V. Angueliev<sup>56</sup>, C. Amaro<sup>57</sup>, T. Anticicic<sup>58</sup>, R. Antillon<sup>59</sup>, S. Antino<sup>60</sup>, K. Antipin<sup>61</sup>, D. Antoš<sup>62</sup>, P. Antonioli<sup>63</sup>, A. Anwar<sup>64</sup>, L. Aphecchia<sup>65</sup>, H. Appelshäuser<sup>66</sup>, S. Arzelli<sup>67</sup>, R. Arco<sup>68</sup>, A. Arment<sup>69</sup>, N. Aronov<sup>70</sup>, R. Arzuffi<sup>71</sup>, T. Arvanitaki<sup>72</sup>, L.C. Arsenau<sup>73</sup>, A. Arzoo<sup>74</sup>, A. Asano<sup>75</sup>, R. Aschmann<sup>76</sup>, R. Asrbeck<sup>77</sup>, T.C. Awes<sup>78</sup>, J. Ayala<sup>79</sup>, M.D. Azmi<sup>80</sup>, S. Babik<sup>81</sup>, M. Bach<sup>82</sup>, A. Badalá<sup>83</sup>, Y.W. Baek<sup>84</sup>, S. Bagnasco<sup>85</sup>, R. Bailhache<sup>86</sup>, K. Bala<sup>87</sup>, A. Baldisseri<sup>88</sup>, A. Balitá<sup>89</sup>, J. Balaž<sup>90</sup>, R. Balaž<sup>91</sup>, G.G. Barnafid<sup>92</sup>, L. Barile<sup>93</sup>, V. Barret<sup>94</sup>, J. Barke<sup>95</sup>, F. Barile<sup>96</sup>, M. Basil<sup>97</sup>, V. Batusov<sup>98</sup>, N. Behtold<sup>99</sup>, B. Bélian<sup>100</sup>, G. Belgin<sup>101</sup>, B. Belyaev<sup>102</sup>, C. Bessada<sup>103</sup>, L.G. Besen<sup>104</sup>, B. Becker<sup>105</sup>, I. Belikov<sup>106</sup>, R. Bellwied<sup>107</sup>, R. Belmont-Morano<sup>108</sup>, A. Belousov<sup>109</sup>, L. Bercini<sup>110</sup>, S. Beroš<sup>111</sup>, I. Beresna<sup>112</sup>, A. Berciu<sup>113</sup>, K. Berdnikow<sup>114</sup>, Y. Berdnikov<sup>115</sup>, L. Bertsch<sup>116</sup>, A. Bhanu<sup>117</sup>, A.K. Bhat<sup>118</sup>, L. Bhanu<sup>119</sup>, N. Bhatt<sup>120</sup>, C. Bhattin<sup>121</sup>, J. Bielecki<sup>122</sup>, A. Bilekova<sup>123</sup>, I. Bimker<sup>124</sup>, F. Bincoletti<sup>125</sup>, A. Bion<sup>126</sup>, F. Bianco<sup>127</sup>, R. Bianco<sup>128</sup>, D. Bhas<sup>129</sup>, C. Bhanu<sup>130</sup>, M. Bichsel<sup>131</sup>, N. Bickel<sup>132</sup>, A. Biedron<sup>133</sup>, H. Beggild<sup>134</sup>, M. Belyukh<sup>135</sup>, J. Belin<sup>136</sup>, L. Belin<sup>137</sup>, M. Beldous<sup>138</sup>, C. Bemporad<sup>139</sup>, M. Boudia<sup>140</sup>, H. Borek<sup>141</sup>, Y. Borshchov<sup>142</sup>, C. Bortolin<sup>143</sup>, S. Boss<sup>144</sup>, L. Bossio<sup>145</sup>, F. Bossi<sup>146</sup>, M. Botje<sup>147</sup>, S. Böttger<sup>148</sup>, G. Boudard<sup>149</sup>, H. Beyer<sup>150</sup>, M. Brann<sup>151</sup>, P. Brann-Manninger<sup>152</sup>, L. Bravin<sup>153</sup>, M. Braganza<sup>154</sup>, T. Bredner<sup>155</sup>, G. Bruckner<sup>156</sup>, R. Brum<sup>157</sup>, R. Bruna<sup>158</sup>, G.R. Bruno<sup>159</sup>, D. Budnikov<sup>160</sup>, H. Buehler<sup>161</sup>, K. Bugay<sup>162</sup>, P. Bunc<sup>163</sup>, O. Busch<sup>164</sup>, Z. Buthe<sup>165</sup>, D. Caffari<sup>166</sup>, X. Cai<sup>167</sup>, H. Cai<sup>168</sup>, E. Caines<sup>169</sup>, E. Caines<sup>170</sup>, P. Camerini<sup>171</sup>, M. Campbell<sup>172</sup>, V. Canas Roman<sup>173</sup>, G.P. Caprini<sup>174</sup>, G. Carrone<sup>175</sup>, E. Caron<sup>176</sup>, W. Caron<sup>177</sup>, K. Caron<sup>178</sup>, A. Casanova Diaz<sup>179</sup>, M. Caselle<sup>180</sup>, J. Castillo Castellanos<sup>181</sup>, J.F. Castillo Hernandez<sup>182</sup>, V. Cattaui<sup>183</sup>, K. Cattaruzza<sup>184</sup>, C. Castejón<sup>185</sup>, P. Causino<sup>186</sup>, V. Chabrier<sup>187</sup>, B. Chang<sup>188</sup>, S. Chaplinski<sup>189</sup>, A. Charpy<sup>190</sup>, J.L. Charvet<sup>191</sup>, S. Chatterjee<sup>192</sup>, S. Chatterjee<sup>193</sup>, M. Cherczak<sup>194</sup>, C. Cheshkov<sup>195</sup>, E. Chyryś<sup>196</sup>, E. Chierici<sup>197</sup>, V. Chibrikov<sup>198</sup>, D.D. Chikhatov<sup>199</sup>, P. Chikhatov<sup>200</sup>, K. Choi<sup>201</sup>, M. Chojnacki<sup>202</sup>, P. Chikobava<sup>203</sup>, C.D. Chisari<sup>204</sup>, P. Christiansen<sup>205</sup>, T. Chujko<sup>206</sup>, F. Chuman<sup>207</sup>, C. Cioba<sup>208</sup>, L. Cifarelli<sup>209</sup>, E. Cifarelli<sup>210</sup>, J. Cifuentes<sup>211</sup>, O. Cifuentes<sup>212</sup>, J.-P. Coffin<sup>213</sup>, S. Coffin<sup>214</sup>, A. Colla<sup>215</sup>, G. Conesa Balbastre<sup>216</sup>, Z. Conesa Balbastre<sup>217</sup>, E.S. Conner<sup>218</sup>, P. Constantin<sup>219</sup>, G. Contino<sup>220</sup>, J.G. Contreras<sup>221</sup>, Y. Corral Morales<sup>222</sup>, T.M. Cormier<sup>223</sup>, P. Corvo<sup>224</sup>, I. Coric<sup>225</sup>, M.R. Cosentino<sup>226</sup>, K. Costa<sup>227</sup>, M.G. Coull<sup>228</sup>, E. Crescio<sup>229</sup>, P. Crosier<sup>230</sup>, E. Cruz<sup>231</sup>, L. Cunqueiro<sup>232</sup>, J. Czopkiewicz<sup>233</sup>, A. Daloz<sup>234</sup>, H.H. Dabagyan<sup>235</sup>, A. Dam<sup>236</sup>, I. Dan<sup>237</sup>, S. Dan<sup>238</sup>, A. Dash<sup>239</sup>, G.O.V. de Barros<sup>240</sup>, A. De Caro<sup>241</sup>, G. de Cataldo<sup>242</sup>, J. de Cevallos<sup>243</sup>, A. De Falco<sup>244</sup>, M. de Gascari<sup>245</sup>, J. de Groot<sup>246</sup>, D. De Greif<sup>247</sup>, A.P. de Haze<sup>248</sup>, N. De Marco<sup>249</sup>, R. de Rooij<sup>250</sup>, S. De Saiz<sup>251</sup>, G. de Vries<sup>252</sup>, H. Debusche<sup>253</sup>, G. Debusche<sup>254</sup>, A. Deloff<sup>255</sup>, V. Demina<sup>256</sup>, E. Dénia<sup>257</sup>, A. Deppman<sup>258</sup>, G. Di Francesco<sup>259</sup>, B. Diklich<sup>260</sup>, A. Diklich<sup>261</sup>, B. Di Raso<sup>262</sup>, C. Di Gliglio<sup>263</sup>, S. Di Liberto<sup>264</sup>, A. Di Mauro<sup>265</sup>, P. Di Nezza<sup>266</sup>, M. Di Palma<sup>267</sup>, L. Di Bari<sup>268</sup>, B. Díaz<sup>269</sup>, T. Diehl<sup>270</sup>, H. Ding<sup>271</sup>, R. Divá<sup>272</sup>, D. Djurkovic<sup>273</sup>, G. da Amaral Valdivieso<sup>274</sup>, V. Dobrev<sup>275</sup>, A. Dobrin<sup>276</sup>, T. Dobrowolski<sup>277</sup>, B. Dönigus<sup>278</sup>, E. Dominguez<sup>279</sup>, D.M.M. Dos<sup>280</sup>, O. Dordic<sup>281</sup>, A.K. Dubey<sup>282</sup>, J. Dubinin<sup>283</sup>, L. Durron<sup>284</sup>, P. Dupieux<sup>285</sup>, A.K. Datta Majumdar<sup>286</sup>, M.R. Datta Majumdar<sup>287</sup>, B. Datta<sup>288</sup>, B. Derschmann<sup>289</sup>, A. De Leo<sup>290</sup>, H. Espagnon<sup>291</sup>, M. Estienne<sup>292</sup>, B. Estienne<sup>293</sup>, S. Evrard<sup>294</sup>, G. Eyyubova<sup>295</sup>, C.W. Falgarone<sup>296</sup>, D. Falck<sup>297</sup>, J. Faivre<sup>298</sup>, B. Falchier<sup>299</sup>, A. Fantoni<sup>300</sup>, M. Fasel<sup>301</sup>, R. Fausch<sup>302</sup>, A. Fedunov<sup>303</sup>, B. Fedkin<sup>304</sup>, Y. Felkin<sup>305</sup>, D. Felz<sup>306</sup>, B. Fealton-Ober<sup>307</sup>, G. Felice<sup>308</sup>, A. Fernández Tellez<sup>309</sup>, Ed. Ferreiro<sup>310</sup>, A. Ferrel<sup>311</sup>, R. Ferretti<sup>312</sup>, M.A.S. Figueroa<sup>313</sup>, R. Fichagna<sup>314</sup>, R. Fifi<sup>315</sup>, E.M. Fijač<sup>316</sup>, E.M. Fijač<sup>317</sup>, M. Fiora<sup>318</sup>, Z. Fodor<sup>319</sup>, S. Focitsch<sup>320</sup>, P. Foka<sup>321</sup>, S. Fokin<sup>322</sup>, F. Fontana<sup>323</sup>.

Published online 11 December 2016

Springer

E. Fragiacomo<sup>134</sup>, M. Fragkiadaki<sup>135</sup>, I. Franksfeld<sup>136</sup>, A. Freitas<sup>137</sup>, I. Fuchs<sup>138</sup>, F. Fursten<sup>139</sup>, C. Furgas<sup>140</sup>, M. Fusco Girard<sup>141</sup>, J.J. Gaardhøje<sup>142</sup>, S. Gaike<sup>143</sup>, M. Gagliardi<sup>144</sup>, A. Gagne<sup>145</sup>, M. Gaiola<sup>146</sup>, P. Ganiou<sup>147</sup>, M.S. Ganti<sup>148</sup>, C. Garabatos<sup>149</sup>, C. García Trapani<sup>150</sup>, J. Gebelka<sup>151</sup>, R. Gemme<sup>152</sup>, M. Germain<sup>153</sup>, A. Ghata<sup>154</sup>, M. Ghete<sup>155</sup>, B. Ghidini<sup>156</sup>, P. Ghosh<sup>157</sup>, G. Ghisla<sup>158</sup>, P. Giacobino<sup>159</sup>, E. Ghidys-Driantes<sup>160</sup>, R. Ghose<sup>161</sup>, P. Gliason<sup>162</sup>, A. Glaz<sup>163</sup>, R. Gomez<sup>164</sup>, H. González Santos<sup>165</sup>, L.H. González-Uribe<sup>166</sup>, P. González-Zamora<sup>167</sup>, S. Gobbo<sup>168</sup>, Y. Gobzar<sup>169</sup>, S. Godwin<sup>170</sup>, H. Godschalk<sup>171</sup>, V. Gotoku<sup>172</sup>, R. Graczyk<sup>173</sup>, A. Greife<sup>174</sup>, A. Grieras<sup>175</sup>, C. Griepker<sup>176</sup>, V. Griepker<sup>177</sup>, A. Griegoryan<sup>178</sup>, B. Griess<sup>179</sup>, N. Griou<sup>180</sup>, P. Gros<sup>181</sup>, J.F. Gruber-Oberlingham<sup>182</sup>, J.-Y. Gruber<sup>183</sup>, R. Gross<sup>184</sup>, C. Guarnaccia<sup>185</sup>, E. Guber<sup>186</sup>, R. Guermat<sup>187</sup>, E. Guercio<sup>188</sup>, K. Gulbenkian<sup>189</sup>, H. Gulbayan<sup>190</sup>, T. Gunji<sup>191</sup>, A. Gupta<sup>192</sup>, R. Gupta<sup>193</sup>, H.-A. Gustafsson<sup>194</sup>, H. Gutbrod<sup>195</sup>, Ø. Haaheim<sup>196</sup>, C. Hadjidakis<sup>197</sup>, M. Haidt<sup>198</sup>, H. Hamaoka<sup>199</sup>, G. Harma<sup>200</sup>, J. Harland-Beck<sup>201</sup>, B.H. Han<sup>202</sup>, J.W. Han<sup>203</sup>, M. Hara<sup>204</sup>, A. Harutyunyan<sup>205</sup>, D. Hasek<sup>206</sup>, D. Hasegan<sup>207</sup>, P. Hasebotoh<sup>208</sup>, A. Hayrapetyan<sup>209</sup>, M. Heide<sup>210</sup>, M. Heide<sup>211</sup>, T. Heikamp<sup>212</sup>, A. Heijboer<sup>213</sup>, C. Hernández<sup>214</sup>, G. Herrera Carrón<sup>215</sup>, N. Herrmann<sup>216</sup>, K.F. Heitland<sup>217</sup>, B. Hicks<sup>218</sup>, A. Hiel<sup>219</sup>, P.T. Hill<sup>220</sup>, B. Hippolyte<sup>221</sup>, T. Horiguchi<sup>222</sup>, Y. Hori<sup>223</sup>, P. Hristov<sup>224</sup>, I. Hristova<sup>225</sup>, S. Hu<sup>226</sup>, S. Huber<sup>227</sup>, T.J. Humanic<sup>228</sup>, D. Hultsch<sup>229</sup>, D.S. Hwang<sup>230</sup>, R. Idoni<sup>231</sup>, J.H. Kang<sup>232</sup>, I. Hleir<sup>233</sup>, P.G. Innocenti<sup>234</sup>, M. Ippolito<sup>235</sup>, M. Irles<sup>236</sup>, C. Ivan<sup>237</sup>, A. Ivano<sup>238</sup>, M. Ivano<sup>239</sup>, V. Ivano<sup>240</sup>, T. Iwasaki<sup>241</sup>, A. Iwasaki<sup>242</sup>, P.M. Jacobs<sup>243</sup>, L. Janczowski<sup>244</sup>, S. Jang<sup>245</sup>, R. Jank<sup>246</sup>, K. Janyalová<sup>247</sup>, C. Jen<sup>248</sup>, S. Jen<sup>249</sup>, L. Jindra<sup>250</sup>, G.T. Jones<sup>251</sup>, B.G. Jones<sup>252</sup>, P. Jovanović<sup>253</sup>, E. Jung<sup>254</sup>, W. Jung<sup>255</sup>, A. Junk<sup>256</sup>, A.B. Kaidelas<sup>257</sup>, S. Kalcher<sup>258</sup>, P. Kallibek<sup>259</sup>, T. Kallibekov<sup>260</sup>, A. Kalisek<sup>261</sup>, A. Kalin<sup>262</sup>, R. Kammermann<sup>263</sup>, K. Kanaki<sup>264</sup>, F. Kang<sup>265</sup>, J.H. Kang<sup>266</sup>, J. Kapitan<sup>267</sup>, V. Kapiri<sup>268</sup>, S. Kapusta<sup>269</sup>, T. Karavicheva<sup>270</sup>, E. Karpechev<sup>271</sup>, A. Kaszian<sup>272</sup>, U. Kebschull<sup>273</sup>, R. Keidel<sup>274</sup>, M.M. Khan<sup>275</sup>, S.A. Khan<sup>276</sup>, A. Khachatryan<sup>277</sup>, Y. Khachatryan<sup>278</sup>, D. Kikola<sup>279</sup>, E. Kilgus<sup>280</sup>, D.J. Kim<sup>281</sup>, D.S. Kim<sup>282</sup>, D.W. Kim<sup>283</sup>, H.N. Kim<sup>284</sup>, J. Kim<sup>285</sup>, J.H. Kim<sup>286</sup>, J.S. Kim<sup>287</sup>, M. Kim<sup>288</sup>, M. Kim<sup>289</sup>, S.H. Kim<sup>290</sup>, S. Kim<sup>291</sup>, Y. Kim<sup>292</sup>, S. Kirseb<sup>293</sup>, I. Kise<sup>294</sup>, S. Kiselev<sup>295</sup>, A. Kishimoto<sup>296</sup>, J.L. Klay<sup>297</sup>, J. Kline<sup>298</sup>, C. Klein-Börsig<sup>299</sup>, M. Kleinwort<sup>300</sup>, A. Klöning<sup>301</sup>, A. Kluge<sup>302</sup>, S. Kluge<sup>303</sup>, K. Koch<sup>304</sup>, B. Koberling<sup>305</sup>, A. Koc<sup>306</sup>, V. Kozlov<sup>307</sup>, N. Kondratyev<sup>308</sup>, A. Korotkiy<sup>309</sup>, E. Korut<sup>310</sup>, H. Koss<sup>311</sup>, M. Kowalek<sup>312</sup>, S. Kotl<sup>313</sup>, K. Kozlov<sup>314</sup>, J. Kratoch<sup>315</sup>, I. Krüker<sup>316</sup>, F. Kramer<sup>317</sup>, J. Kraus<sup>318</sup>, A. Krawinkel<sup>319</sup>, E. Krawinkel<sup>320</sup>, M. Krüger<sup>321</sup>, D. Krüger<sup>322</sup>, M. Krüger<sup>323</sup>, E. Krüger<sup>324</sup>, M. Krzewicki<sup>325</sup>, Y. Kucheryav<sup>326</sup>, C. Kuhn<sup>327</sup>, P.G. Kuijer<sup>328</sup>, L. Kumar<sup>329</sup>, N. Kumar<sup>330</sup>, R. Kupczak<sup>331</sup>, P. Kuznetsov<sup>332</sup>, A. Kurupin<sup>333</sup>, A.N. Kurupin<sup>334</sup>, A. Kurupin<sup>335</sup>, S. Kuspi<sup>336</sup>, V. Kuspi<sup>337</sup>, M. Kuznetsov<sup>338</sup>, H. Kwara<sup>339</sup>, M.J. Kwiat<sup>340</sup>, Y. Kwiat<sup>341</sup>, R. La Banca<sup>342</sup>, S. Lackner<sup>343</sup>, P. Ladrón de Guevara<sup>344</sup>, V. Lafage<sup>345</sup>, C. Laf<sup>346</sup>, C. Lara<sup>347</sup>, D.T. Larson<sup>348</sup>, G. Lazzarotti<sup>349</sup>, C. Lazzaroni<sup>350</sup>, Y. Le Bourne<sup>351</sup>, M. Le Ber<sup>352</sup>, H. Lee<sup>353</sup>, K.S. Lee<sup>354</sup>, K.C. Lee<sup>355</sup>, J. Lehto<sup>356</sup>, M. Lehto<sup>357</sup>, M. Lehto<sup>358</sup>, J. Lehto<sup>359</sup>, V. Lehto<sup>360</sup>, H. León<sup>361</sup>, J. León Martínez<sup>362</sup>, H. León Vargas<sup>363</sup>, P. León<sup>364</sup>, Y. Li<sup>365</sup>, R. Lietava<sup>366</sup>, S. Lindal<sup>367</sup>, V. Lindel<sup>368</sup>, C. Lippmann<sup>369</sup>, M.A. Lina<sup>370</sup>, O. Litratońka<sup>371</sup>, L. Liu<sup>372</sup>, V. Loginov<sup>373</sup>, S. Loh<sup>374</sup>, X. Lopez<sup>375</sup>, M. López Noriega<sup>376</sup>, R. López-Ramírez<sup>377</sup>, R. López Torres<sup>378</sup>, G. Lovhalden<sup>379</sup>, A. Loma Feljo Suarez<sup>380</sup>, S. Lu<sup>381</sup>, M. Luszczak<sup>382</sup>, G. Luparello<sup>383</sup>, L. Lujan<sup>384</sup>, J.-R. Lutz<sup>385</sup>, M. Luvizotto<sup>386</sup>, K. Ma<sup>387</sup>, R. Ma<sup>388</sup>, D.M. Madhavadhan<sup>389</sup>, A. Mahdavi<sup>390</sup>, M. Magas<sup>391</sup>, A. Mahajan<sup>392</sup>, D.P. Mahapatra<sup>393</sup>, A. Maire<sup>394</sup>, I. Makhsoum<sup>395</sup>, D. Mal'Kevich<sup>396</sup>, M. Malchev<sup>397</sup>, I. Malchenko<sup>398</sup>, M. Malck<sup>399</sup>, T. Malinská<sup>400</sup>, P. Malinská<sup>401</sup>, A. Malinin<sup>402</sup>, L. Malinova<sup>403</sup>, V. Malinova<sup>404</sup>, F. Mams<sup>405</sup>, V. Manzari<sup>406</sup>, Y. Mao<sup>407</sup>, J. Marco<sup>408</sup>, G.V. Margagliotti<sup>409</sup>, A. Margoni<sup>410</sup>, A. Marin<sup>411</sup>, I. Martiniello<sup>412</sup>, P. Martinengo<sup>413</sup>, M.L. Martinez<sup>414</sup>, A. Martínez Revilla<sup>415</sup>, G. Martiniere Garcia<sup>416</sup>, Y. Maruyama<sup>417</sup>, A. Marzani Chica<sup>418</sup>, S. Mascheretti<sup>419</sup>, M. Masera<sup>420</sup>, M. Masetti<sup>421</sup>, A. Masetti<sup>422</sup>, L. Matarrese<sup>423</sup>, M. Matarrese<sup>424</sup>, A. Matarrese<sup>425</sup>, Z.L. Mathews<sup>426</sup>, B. Mattoz Tavara<sup>427</sup>, A. Matsuzaki<sup>428</sup>, D. Mavrouk<sup>429</sup>, G. Mazza<sup>430</sup>, M.A. Mazza<sup>431</sup>, F. Meddi<sup>432</sup>, A. Merchlitz-Rocha<sup>433</sup>, P. Merleix Laxaux<sup>434</sup>, M. Mesiti<sup>435</sup>, J. Mercado Pérez<sup>436</sup>, P. Meres<sup>437</sup>, Y. Miska<sup>438</sup>, A. Michalek<sup>439</sup>, S. Mikhaleva<sup>440</sup>, J. Mikhaleva<sup>441</sup>, E. Minder<sup>442</sup>, A. Mischke<sup>443</sup>, D. Miśkowiec<sup>444</sup>, C. Miñi<sup>445</sup>, K. Minoguchi<sup>446</sup>, J. Mlynar<sup>447</sup>, B. Mohanty<sup>448</sup>, E. Molnar<sup>449</sup>, M.M. Mondal<sup>450</sup>, L. Montaño Zedeno<sup>451</sup>, M. Monteno<sup>452</sup>, E. Montes<sup>453</sup>, M. Morand<sup>454</sup>, S. Moric<sup>455</sup>, A. Morselli<sup>456</sup>, Y. Moshkova<sup>457</sup>, V. Mousaev<sup>458</sup>, E. Mouta<sup>459</sup>, S. Mubari<sup>460</sup>, H. Müller<sup>461</sup>, M.G. Mühlbauer<sup>462</sup>, J. Mura<sup>463</sup>, L. Mura<sup>464</sup>, A. Mura<sup>465</sup>, R.K. Nandi<sup>466</sup>, R. Nandi<sup>467</sup>, E. Nappi<sup>468</sup>, F. Narech<sup>469</sup>, S. Narić<sup>470</sup>, T.K. Nayak<sup>471</sup>, S. Nazarenko<sup>472</sup>, G. Nazarov<sup>473</sup>, A. Nedavkin<sup>474</sup>, E. Nefedov<sup>475</sup>, J. Newby<sup>476</sup>, A. Niazov<sup>477</sup>, M. Niczko<sup>478</sup>, H.S. Nielsen<sup>479</sup>, S. Nikolic<sup>480</sup>, V. Nikolic<sup>481</sup>, S. Nikulin<sup>482</sup>, V. Nikulin<sup>483</sup>, B.S. Nilsen<sup>484</sup>, M.S. Nilsen<sup>485</sup>, E. Nisferati<sup>486</sup>, P. Niswonger<sup>487</sup>, G. Nooren<sup>488</sup>, N. Novitskiy<sup>489</sup>, A. Nyffeler<sup>490</sup>, C. Nygaard<sup>491</sup>, A. Nyiri<sup>492</sup>, J. Nystrand<sup>493</sup>, A. Ochirov<sup>494</sup>, G. Odysse<sup>495</sup>, H. Oeschler<sup>496</sup>, M. Ogorodnikov<sup>497</sup>, K. Okada<sup>498</sup>, V. Okada<sup>499</sup>, M. Okunev<sup>500</sup>, J. Olieriva<sup>501</sup>, C. Oppedisano<sup>502</sup>, F. Orlandi<sup>503</sup>, A. Ortiz Velázquez<sup>504</sup>, G. Ortona<sup>505</sup>, C. Ostapenko<sup>506</sup>, A. Ostapenko<sup>507</sup>, E. Otrelin<sup>508</sup>, I. Otterman<sup>509</sup>, P. Otrassini<sup>510</sup>, I. Otterlund<sup>511</sup>, J. Otrorowski<sup>512</sup>, G. Östberg<sup>513</sup>, K. Oyama<sup>514</sup>, K. Ozawa<sup>515</sup>, V. Pachmayr<sup>516</sup>.



- <sup>4</sup>Physics Department, University of Arizona, Tucson, Illinois
- <sup>5</sup>Departmento de Física, M. Sclater and Sezione INFN, Bari, Italy
- <sup>6</sup>Sezione INFN, Bari, Italy
- <sup>7</sup>China Institute of Atomic Energy, Beijing, China
- <sup>8</sup>Department of Physics and Technology, University of Bergen, Bergen, Norway
- <sup>9</sup>School of Engineering, Boston University College, Boston, Norway
- <sup>10</sup>Lawrence Berkeley National Laboratory, Berkeley, CA, USA
- <sup>11</sup>Institute of Physics, Bhubaneswar, India
- <sup>12</sup>National Physics and Astronomy, University of Birmingham, Birmingham, UK
- <sup>13</sup>Departmento di Fisica and Nazionale di Fisica INFN, Bologna, Italy
- <sup>14</sup>Sezione INFN, Bologna, Italy
- <sup>15</sup>Faculty of Mathematics, Physical Informatics, Chemical University, Bratislava, Slovakia
- <sup>16</sup>Instituto de Física de São Carlos, São Carlos, Brazil
- <sup>17</sup>Max Planck Institute for Physics and Division Engineering, Dachau, Germany
- <sup>18</sup>Wigner Research Institute for Particle and Nuclear Physics, Hungarian Academy of Sciences, Budapest, Hungary
- <sup>19</sup>Department of Physics and Astronomy, University of Cambridge, Cambridge, UK
- <sup>20</sup>Sezione INFN, Cagliari, Italy
- <sup>21</sup>Universidade Federal de Campinas (UNICAMP), Campinas, Brazil
- <sup>22</sup>Physics Department, University of Cape Town, Theoretical Laboratories, Cape Town, South Africa
- <sup>23</sup>Departmento di Fisica and Sezione INFN, Università di Ferrara, Ferrara, Italy
- <sup>24</sup>Sezione INFN, Ferrara, Italy
- <sup>25</sup>Physics Department, Fermi University, Ginevra, Italy
- <sup>26</sup>Abteilung der Physik, Corporate (LPC), German University, Universität Bonn, CBNS INFN, Clermont-Ferrand, France
- <sup>27</sup>Department of Physics, Ohio State University, Columbus, OH, USA
- <sup>28</sup>Statens Fysiske Institut, University of Copenhagen, Copenhagen, Denmark
- <sup>29</sup>The Horia Hulubei National Institute of Nuclear Physics, Bucharest, Romania
- <sup>30</sup>Physics Department, Georgia Institute of Technology, Atlanta, GA, USA
- <sup>31</sup>Universidad Autónoma de San Luis Potosí, México
- <sup>32</sup>Max Planck Institute (MPI) for Nuclear Physics, Heidelberg, Germany
- <sup>33</sup>Max Planck Institute, Technische Universität München, Garching, Germany
- <sup>34</sup>Wayne State University, Detroit, MI, USA
- <sup>35</sup>Max Planck Institute for Nuclear Physics (MPI), Heidelberg, Germany
- <sup>36</sup>Max Planck Institute for Advanced Studies, Johann Wolfgang Goethe Universität Frankfurt, Frankfurt, Germany
- <sup>37</sup>Centre für Kernphysik, Johann Wolfgang Goethe Universität Frankfurt, Frankfurt, Germany
- <sup>38</sup>Abteilung Mathematik, Physik, INFN, Ferrara, Italy
- <sup>39</sup>Protonic Nuclear Physics Institute, Guelma, Algeria
- <sup>40</sup>European Organization for Nuclear Research (CERN), Geneva, Switzerland
- <sup>41</sup>Laboratoire de Physique Subatomique et de Cosmologie (LUSC), Université Joseph Fourier, CNRS-CEA, Institut Polytechnique de Grenoble, Grenoble, France
- <sup>42</sup>Centro de Aplicaciones Tecnológicas y Desarrollo Nuclear (CEADEN), Havana, Cuba
- <sup>43</sup>Max Planck Institute für Physik, Werner-Heisenberg Institut, München, Germany
- <sup>44</sup>Physikalisches Institut, Ruprecht-Karls-Universität Heidelberg, Heidelberg, Germany
- <sup>45</sup>Osaka University, Suita, Japan
- <sup>46</sup>University of Houston, Houston, TX, USA
- <sup>47</sup>Rayon Department, University of Kagoshima, Japan, India
- <sup>48</sup>Physics Department, University of Jammu, Jammu, India
- <sup>49</sup>High Energy Institute of Physics (HEP) and University of Jyväskylä, Jyväskylä, Finland
- <sup>50</sup>Kangnung National University, Kangnung, South Korea
- <sup>51</sup>Scientific Research Technological Institute of Instrument Engineering, Kharkov, Ukraine
- <sup>52</sup>Reguljovskij Institute for Theoretical Physics, Kiev, Ukraine
- <sup>53</sup>University of Tennessee, Knoxville, TN, USA
- <sup>54</sup>Saha Institute of Nuclear Physics, Kolkata, India
- <sup>55</sup>Variable Energy Cyclotron Centre, Kolkata, India
- <sup>56</sup>Fachbereich für Physik, Köln, Germany
- <sup>57</sup>Faculty of Science, Chulalongkorn University, Bangkok, Thailand
- <sup>58</sup>Institute of Experimental Physics, Slovak Academy of Sciences, Košice, Slovakia
- <sup>59</sup>Laboratoire National de Physique, INFN, Lignano, Italy
- <sup>60</sup>Lawrence Livermore National Laboratory, Livermore, CA, USA
- <sup>61</sup>Institute of Experimental High Energy Physics, Ministry of Energy, Lund, Sweden
- <sup>62</sup>Universitat de València, IFAE-CSIC, Institut de Física Corpuscular, Valencia, Spain
- <sup>63</sup>Centro de Investigaciones Científicas y Tecnológicas (CITEC), Madrid, Spain
- <sup>64</sup>Centro de Investigaciones y de Estudios Científicos (CINVESTAV), Mexico City and Merida, Mexico
- <sup>65</sup>Instituto de Ciencias Nucleares, Universidad Nacional Autónoma de México, Mexico City, Mexico
- <sup>66</sup>Centro de Física, Universidad Nacional Autónoma de México, Mexico City, Mexico
- <sup>67</sup>Institute for Nuclear Research, Academy of Sciences, Moscow, Russia

Prog. Phys. 1:42

- <sup>48</sup>Institute for Theoretical and Experimental Physics, Moscow, Russia  
<sup>49</sup>Moscow Engineering Thechnical Institute, Moscow, Russia  
<sup>50</sup>Russian Research Center Kurchatov Institute, Moscow, Russia  
<sup>51</sup>Lakshmi Institute of Technology, Mysore, India  
<sup>52</sup>Physikalisches Institut, Westfälische Wilhelms-Universität Münster, Münster, Germany  
<sup>53</sup>SUBATECH, Centre for Studies of Nuclear, Université de Nantes, CNRS-IN2P3, Nantes, France  
<sup>54</sup>Yale University, New Haven, CT, USA  
<sup>55</sup>Institut National für Nuklearphysik, Karlsruhe, Germany  
<sup>56</sup>High Energy Physics Laboratory, Oak Ridge, TN, USA  
<sup>57</sup>Institutul Fizicilor Nucleare din Oradea (IFNO), Universitatii "Babeş-Bolyai", Oradea, Romania  
<sup>58</sup>Department of Physics, University of Oslo, Oslo, Norway  
<sup>59</sup>Dipartimento di Fisica dell'Università del Piemonte Orientale (D.F.O.), Alessandria, Italy  
<sup>60</sup>Scienze INFN, Ferrara, Italy  
<sup>61</sup>Faculty of Applied Sciences and Electrical Engineering, Czech Technical University in Prague, Prague, Czech Republic  
<sup>62</sup>Institute of Physics, Academy of Sciences of the Czech Republic, Prague, Czech Republic  
<sup>63</sup>Institute for High Energy Physics, Gatchina, Russia  
<sup>64</sup>Universidad Nacional Autónoma de México, México, Mexico  
<sup>65</sup>Yonsei National University, Seoul, South Korea  
<sup>66</sup>Nuclear Physics Institute, Academy of Sciences of the Czech Republic, Brno, Czech Republic  
<sup>67</sup>Dipartimento di Fisica dell'Università di Cagliari and INFN, Cagliari, Italy  
<sup>68</sup>Scienze INFN, Roma, Italy  
<sup>69</sup>Commissariat à l'Énergie Atomique (CEA), Saclay, France  
<sup>70</sup>Department of Physics, E.N. Demidov' s University and INFN, Salerno, Italy  
<sup>71</sup>California Polytechnic State University, San Luis Obispo, CA, USA  
<sup>72</sup>Departamento de Física de Partículas and IGME, Universidad de Santiago de Compostela, Santiago de Compostela, Spain  
<sup>73</sup>Chalkidiki Nuclear Center (CNC), Sifakia, Greece  
<sup>74</sup>Central Institute Nuclear Center (CIN), Szeged, Hungary  
<sup>75</sup>Department of Physics, Sejong University, Seoul, South Korea  
<sup>76</sup>Yonsei University, Seoul, South Korea  
<sup>77</sup>Technical University of Split (TFS), Split, Croatia  
<sup>78</sup>V. Pokrovskii Institute for Physics, St. Petersburg State University, St. Petersburg, Russia  
<sup>79</sup>Institut für Experimentelle Kernphysik (IKP), Universität Wuppertal, CNRS-IN2P3, Wuppertal, Germany  
<sup>80</sup>University of Tokyo, Tokyo, Japan  
<sup>81</sup>Dipartimento di Fisica Sperimentale dell'Università del Piemonte Orientale (D.F.S.), Torino, Italy  
<sup>82</sup>Scienze INFN, Turin, Italy  
<sup>83</sup>Dipartimento di Fisica dell'Università del Piemonte Orientale (D.F.), Alessandria, Italy  
<sup>84</sup>Scienze INFN, Trieste, Italy  
<sup>85</sup>University of Turku, Turku, Finland  
<sup>86</sup>Institute for Subatomic Physics - Utrecht University, Utrecht, The Netherlands  
<sup>87</sup>Szchhe Institute for Nuclear Studies, Warsaw, Poland  
<sup>88</sup>Warsaw University of Technology, Warsaw, Poland  
<sup>89</sup>Purdue University, West Lafayette, IN, USA  
<sup>90</sup>Universität Wuppertal, Wuppertal, Germany  
<sup>91</sup>High Energy Physics Laboratory, Wilson, Ohio  
<sup>92</sup>Instituto Tecnológico de Estudios Superiores de Occidente, Toluca, Mexico  
<sup>93</sup>Rudolf Peierls Institute, Jülich, Germany

Received 18 November 2009 / Revised 1 December 2009  
 © CERN 2014. This article is published with open access at [Springerlink.com](http://Springerlink.com)

<sup>7</sup>email: [jagers@skf.in2p3.fr](mailto:jagers@skf.in2p3.fr)

<sup>8</sup>Also at Laboratoire de Physique Corpusculaire (LPC), Commissariat à l'énergie Atomique (CEA), CNRS-IN2P3, Clermont-Ferrand, France

<sup>9</sup>Also at Institut National für Advanced Studies, Technische Universität Chemnitz-Paradeisberg, Chemnitz, Germany

<sup>10</sup>Now at INFN, Padova, Italy

<sup>11</sup>Now at Institut für Wasser- und Energieeffizienz (IWE) Helmholtz-Zentrum für Wasserstoff-Energie, Darmstadt, Germany

<sup>12</sup>Physikalisches Institut für Experimentelle Nuklearphysik, Universität Würzburg, Würzburg, Germany

<sup>13</sup>Now at Physics Department, University of Cape Town, Rondebosch, Cape Town, South Africa

<sup>14</sup>Now at Institut National für Physics and Nuclear Engineering, Bucharest, Romania

<sup>15</sup>Also at University of Houston, Houston, TX, USA

<sup>16</sup>Faculty of Science, P.J. Štefánik University, Comenius, Slovakia

<sup>17</sup>Now at European Organization for Nuclear Research (CERN), Geneva, Switzerland

<sup>18</sup>Now at Helmholtz Institute of Physics (HIP) and University of Jyväskylä, Jyväskylä, Finland

**Abstract** On 26th November 2009, during the early commissioning of the CERN Large Hadron Collider (LHC), two counter-rotating proton bunches were circulated for the first time consistently in the machine, at the LHC injection energy of 450 GeV per beam. Although the proton intensity was very low, with only one filled bunch per beam, and no systematic attempt was made to optimize the collision optics, all LHC experiments reported a number of collision candidates. In the ALICE experiment, the collision region was centred very well in both the longitudinal and trans-

verse directions and 264 events were recorded in coincidence with the two passing proton bunches. 15 events were immediately reconstructed and analyzed both online and offline. We have used these events to measure the pseudorapidity density of charged primary particles in the central region. In the range  $|\eta| < 0.5$ , we obtain  $dN_{ch}/d\eta = 5.10 \pm 0.13(\text{stat.}) \pm 0.22(\text{sys.})$  from isolated interactions, and  $dN_{ch}/d\eta = 3.51 \pm 0.15(\text{stat.}) \pm 0.22(\text{sys.})$  for non-single diffractive interactions. These results are consistent with previous measurements in proton-antiproton interactions at the same centre-of-mass energy at the CERN SppS collider. They also illustrate the excellent functioning and rapid progress of the LHC accelerator, and of both the hardware and software of the ALICE experiment, in this early start-up phase.

<sup>1</sup>Now at Institut für Experimentelle Physik, Albert-Ludwigs-Universität, Hebesstraße 11, D-78106 Freiburg, Germany

<sup>2</sup>Now at INFN, Frascati, Italy

<sup>3</sup>Now at Institut für Experimentelle Physik, Westfälische Wilhelms-Universität Münster, Germany

<sup>4</sup>Now at University of Technology and Applied Sciences of Valencia, Valencia, Spain

<sup>5</sup>Slater Laboratory Lawrence Berkeley Laboratory, Livermore, CA, USA

<sup>6</sup>Also at Lawrence Livermore National Laboratory (LLNL), University of California, Livermore, CA, USA

<sup>7</sup>Now at Dipartimento di Fisica, Università di Cagliari, Università Ca' Foscari Venezia, Italy

<sup>8</sup>Now at

<sup>9</sup>Now at Yale University, New Haven, CT, USA

<sup>10</sup>Now at University of Tsukuba, Tsukuba, Japan

<sup>11</sup>Also at Centro Fermi, Corso Sallustiana 156, Roma, Italy

<sup>12</sup>Now at Laboratoire de Physique Subatomique et de Cosmologie (LPSC), Université Joseph Fourier, CNRS-IN2P3, Laetitia Poljackova, rue de l'Université, Grenoble, France

<sup>13</sup>Now at Dipartimento di Fisica, Sperimentale (INFN) Fisica and Sezione INFN, Turin, Italy

<sup>14</sup>Now at Physics Department, Oregon University, Umatilla, OR, USA

<sup>15</sup>Now at Centre National d'Énergie Atomique, INFN, Saclay, France

<sup>16</sup>Also at Department of Physics, University of York, York, England

<sup>17</sup>Now at Physikalisches Institut, Universität Köln, Germany, Heidelberg, Germany

<sup>18</sup>Now at Institut für Experimentelle Physik, Westfälische Wilhelms-Universität Münster, Germany

<sup>19</sup>Now at Department of Physics and Technology, University of Botswana, Gaborone, Botswana

<sup>20</sup>Now at Physics Department, University of Athens, Athens, Greece

<sup>21</sup>Also at Institut für Experimentelle Physik, Westfälische Wilhelms-Universität Münster, Münster, Germany

<sup>22</sup>Now at SURATECH, Ecole des Mines de Nantes, Université de Nantes, CNRS-IN2P3, Nantes, France

<sup>23</sup>Now at Institut de Física d'Espai i Temps (IFT) Institut de Física d'Espai i Temps, Spain

<sup>24</sup>Now at Centre de Calcul INFN, Lecce, France

<sup>25</sup>Now at INFN, Energy Conversion Center, Bologna, Italy

<sup>26</sup>Also at Dipartimento di Fisica dell'Università and Sezione INFN, Padova, Italy

<sup>27</sup>Also at Sezione INFN, Bologna, Italy

## 1 Introduction

The very first proton-proton collisions at Point 5 of the CERN Large Hadron Collider (LHC) [1] occurred in the afternoon of 26th November 2009, at a centre-of-mass energy  $\sqrt{s} = 900$  GeV, during the commissioning of the accelerator. This publication, based on 264 events recorded in the ALICE detector [2] on that day, describes a determination of the pseudorapidity density of charged primary particles<sup>1</sup>  $dN_{ch}/d\eta(d\eta = -\ln|\tan(\theta/2)|)$ , where  $\theta$  is the polar angle with respect to the beam line) in the central pseudorapidity region. The purpose of this study is to compare with previous measurements for proton-antiproton ( $p\bar{p}$ ) collisions at the same energy [3], and to establish a reference for comparison with forthcoming measurements at higher LHC energies.

This event sample, selected with our trigger, contains three different classes of inelastic interactions, i.e. collisions where new particles are produced: non-diffractive, single-diffractive, and double-diffractive.<sup>2</sup> Repeatedly we cannot distinguish between these classes, which, however, are selected by our trigger with different efficiencies.<sup>3</sup>

<sup>1</sup>Here, primary particles are defined as those particles produced in the collision and not decay products, except protons from weak decays of strange particles such as  $K^0$  and  $\Lambda$ .

<sup>2</sup>Inelastic processes are usually divided into these classes depending on the first of the interacting protons. If one (both) incoming beam particles are scattered into a high angle state, the process is called single (double) diffractive; otherwise, the events are classified as non-diffractive. Particles emitted in diffractive reactions are usually found at smaller angles to that of the central proton.

<sup>3</sup>We estimate the trigger efficiencies for each class using the pseudorapidity information provided by Monte Carlo generators; the values may be up to a factor of two between classes and are listed in Sect. 3. The relative efficiencies of each class taken from published data are not used.

Fig. 7. Fig. 7. 7

In order to compare our data with those of other experiments, we provide the result with two different normalizations: the first one (NDC) corresponds to the sum of all inelastic interactions and corrects the trigger bias individually for all event classes, by weighting them, each with its own estimated trigger efficiency and abundance. The second normalization (non-single-diffractive or NSD) applies this correction for non-diffractive and double-diffractive processes only, while averaging, on average, the single-diffractive contribution.

Multiplicity production is rather successfully described by phenomenological models with Pomeron exchange, which dominates at high energies [8, 13]. These models relate the energy dependence of the total cross section to that of the multiplicity production using a small number of parameters, and are the basis for several Monte Carlo event generators describing soft hadron collisions (see for example [12, 15]). According to these models, it is expected that the charged-particle density increases by a factor 1.7 and 1.9 when raising the LHC centre-of-mass energy from 300 GeV to 7 and 14 TeV respectively (i.e. intermediate and nominal LHC energies). The difference in charged-particle densities between  $p\bar{p}$  and  $pp$  interactions is predicted to decrease as  $1/\sqrt{s}$  at high energies [17]. This difference was last measured at the CERN ISR to be in the range 1.5–2% [18, 19] at  $\sqrt{s} = 29$  GeV. Extrapolating these values to  $\sqrt{s} = 900$  GeV, one obtains a very small difference of about 0.1–0.2%. Therefore, we will compare our measurement in counting  $p\bar{p}$  data and also to different Monte Carlo models.

This article is organized as follows: Sect. 2 describes the experimental conditions during data taking; the main features of the ALICE detector subsystems used for this analysis are described in Sect. 3; Sect. 4 is dedicated to the event selection and data analysis; the results are discussed in Sect. 5 and Sect. 6 contains the conclusion.

## 2 LHC and the run conditions

The LHC, built at CERN in the circular tunnel of 27 km circumference previously used by the Large Electron-Positron collider (LEP), will provide the highest energy ever achieved with particle accelerators. It is designed to collide two counter-propagating beams of protons or heavy ions. The nominal centre-of-mass energy for proton-proton collisions is 14 TeV. However, collisions can be obtained down to  $\sqrt{s} = 900$  GeV, which corresponds to the beam injection energy.

The results from the first proton-proton collisions presented here were obtained during the early commissioning phase of the LHC, when two proton bunches were circulating for the first time consecutively in the machine. The bunches used were the so-called “pilot bunches” (low intensity bunches used during machine commissioning, with

a few  $10^9$  protons per bunch). The two beams were brought into the nominal position for collisions without a specific attempt to maximize the interaction rate. The nominal rms size of FCC beams at injection energy is about 300  $\mu\text{m}$  in the transverse direction and 10.5 cm in the longitudinal (z-axis) direction. However, at this early stage, the beam parameters can deviate from these nominal values, they were not assessed for the fill used in this analysis. For the position fill, for which the longitudinal size was measured, it was found to be stable with an rms of about 8 cm. Assuming Gaussian beam profiles, the transverse region should be smaller than the beam size by a factor of  $\sqrt{2}$  in all directions.

Shortly after circulating beams were established, the ALICE data acquisition system [20, 21] started collecting events with a trigger based on the Silicon Pixel Detector (SPD), requiring two or more hits in the SPD in coincidence with the passage of the non-colliding bunches as inferred from beam pickup detectors. As a precaution, only a small subset of the detector subsystems, including the silicon tracking detectors, and the accelerator trigger system, was turned on, in order to assess the beam conditions provided by the LHC.

The trigger rate was measured just before collisions with the same trigger conditions. Without beams we measured a rate of  $3 \times 10^{-4}$  Hz (in coincidence with one bunch crossing interval per orbit). In coincidence with the passage of the bunch of one circulating beam the rate was 0.006 Hz. As soon as the second beam was injected in the accelerator, the event rate increased significantly, to 0.11 Hz. The first event that was analysed and displayed in the control room by the online reconstruction software AliRoot [22] running in online mode is shown in Fig. 1. This tracked approximately the barely anticipated start of the physics exploitation of the ALICE experiment.<sup>4</sup> The online reconstruction software implemented in the High-Level Trigger (HLT) computer farm [23] also analysed the events in real time and calculated the vertex position of the collected events, shown in Fig. 2. The distributions are very narrow in the transverse plane (sub-millimetric, including contributions from detector resolution and residual misalignment), of about the expected size in the longitudinal direction and well positioned with respect to the nominal centre of the ALICE detector. This provided immediate evidence that a substantial fraction of the events corresponded to collisions between the protons of the two counter-propagating beams.

After 45 minutes, the two beams were dumped in order to proceed with the LHC commissioning programme. In total, 284 events were triggered and recording this short, but important, first run of the ALICE experiment with colliding beams.

<sup>4</sup>The more slightly delayed start of data taking and therefore missed the first few events.

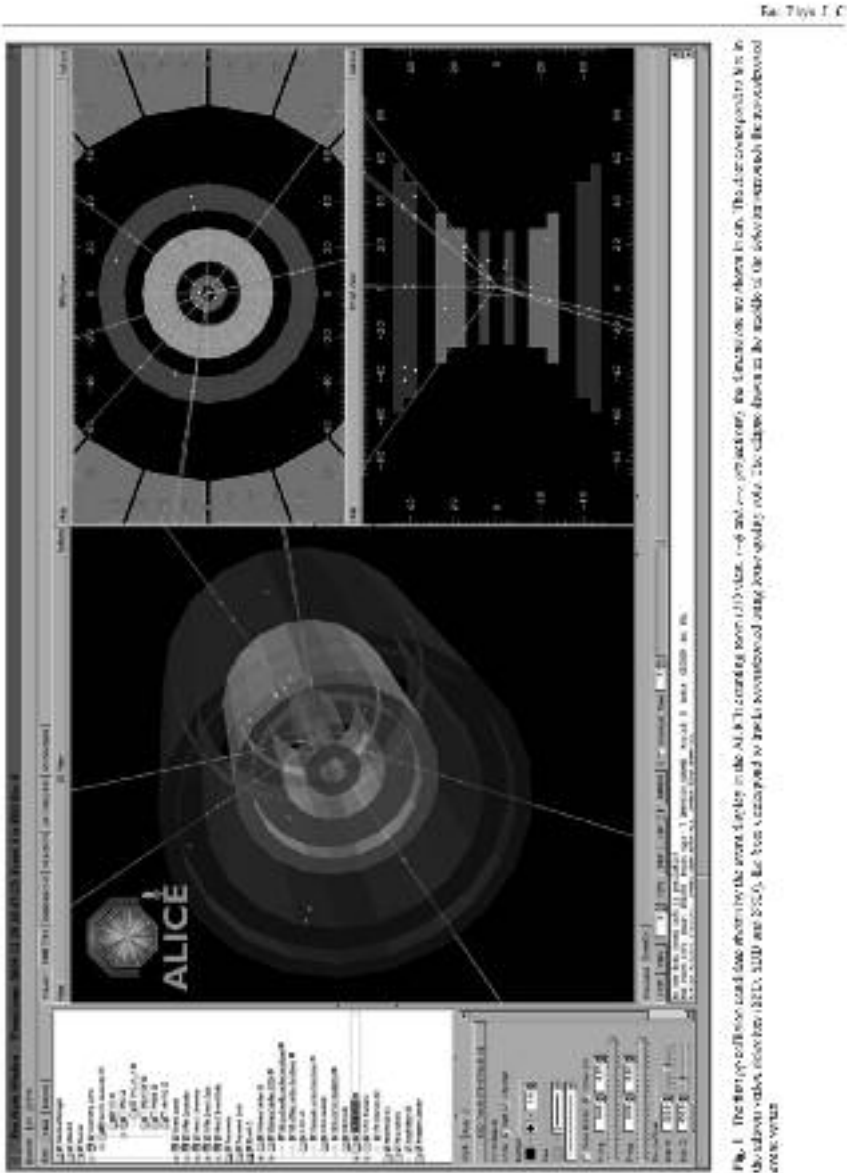


Fig. 2. (Cont.)

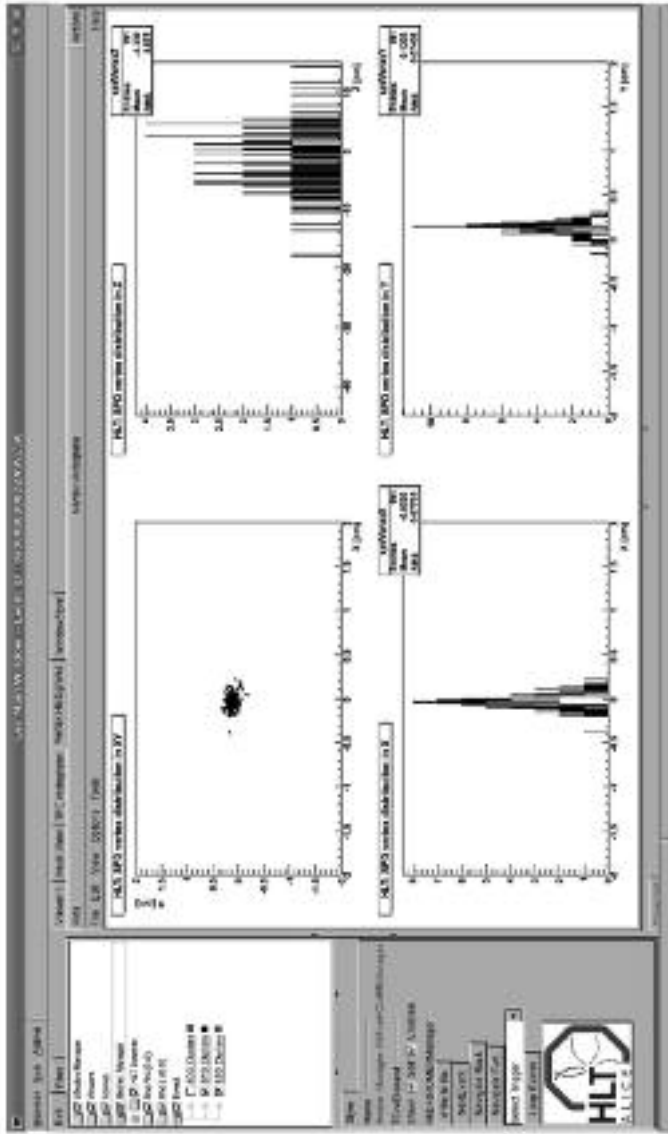


Fig. 2. (Cont.) The histograms show the number distribution of the variables E, F, R, and T for the 1893 data. The scatter plot shows the relationship between the variables E and F. The histograms are arranged in a 2x2 grid. The top-left histogram is titled 'NLS 1893 number distribution in E', the top-right 'NLS 1893 number distribution in F', the bottom-left 'NLS 1893 number distribution in R', and the bottom-right 'NLS 1893 number distribution in T'. The scatter plot is located in the center of the interface.

Fig. 1.10

### 3 The ALICE experiment

ALICE, designed as the dedicated heavy-ion experiment at the LHC, also has excellent performance for proton-proton interactions [24, 25]. The experiment consists of a large number of detector subsystems (23) inside a solenoidal magnet ( $B = 0.5$  T). The magnet was off during this run.

During the several months of running with cosmic rays in 2008 and 2009, all of the ALICE detector subsystems were extensively commissioned, calibrated and used for data taking [26–30]. Data were collected for an initial alignment of the parts of the detector that had sufficient exposure to the mostly vertical cosmic-ray flux. Data were also taken during various LHC injection tests to perform timing measurements and other calibrations.

Data were taken place at the center of the ALICE detector, inside a beryllium vacuum beam pipe (7 cm in radius and 800  $\mu\text{m}$  thick). The tracking system in the ALICE central barrel covers the full azimuthal range in the pseudorapidity window  $|\eta| < 0.9$ . It has been designed to cope with the highest charged-particle densities expected in central Pb-Pb collisions. The following four detector subsystems were active during data taking and were used in this analysis:

- The Silicon Pixel Detector (SPD) consists of two cylindrical layers with radii of 3.9 and 7.6 cm and has about 9.5 million pixels of size  $50 \times 425 \mu\text{m}^2$ . It covers the pseudorapidity range  $|\eta| < 2$  and  $|\phi| < 1.4$  for the inner and outer layers respectively, for particles originating at the center of the detector. The effective  $\phi$ -acceptance is larger due to the longitudinal spread of the position of the interaction vertex. The detector is read out by custom-designed ASICs bump-biased directly on silicon pads. Each chip contains 8192 channels and also provides a fast trigger signal if at least one of its pixels is hit. The trigger signals from all 128 chips are then combined in a programmable logic unit, which provides a level-0 trigger signal to the central trigger processor. The total thickness of the SPD amounts to about 2.5% of a radiation length. About 83% of the channels were operational for particle detection and 77% of the chips were used in the trigger logic. The SPD was aligned using cosmic-ray tracks collected during 2008 [31], and the residual misalignment was estimated to be below 10  $\mu\text{m}$  for the modules well covered by mostly vertical tracks. The modules on the sides are likely to be affected by larger residual misalignments.

The Silicon Drift Detector (SDD) consists of two cylindrical layers at radii of 15.0 and 23.9 cm and covers the region  $|\eta| < 0.9$ . It is composed of 260 sensors with an internal voltage divider providing a drift field of 800 V/cm and MCMs charge receptors for slow measurement of the drift speed via dedicated collection triggers.

The charge signal of each of the 120,000 collection anodes, arranged with a pitch of 294  $\mu\text{m}$ , is sampled every 50 ns by an ADC in the front-end electronics. The total thickness of the SDD layers (including mechanical supports and front-end electronics amounting to 24% of a radiation length). About 92% of the anodes were fully operational.

- The two layers of the double-sided Silicon Strip Detector (SSD) are located at radii of 38 and 63 cm respectively, covering  $|\eta| < 0.97$ . The SSD consists of 1698 sensors with a strip pitch of 97  $\mu\text{m}$  and a stereo angle of 35 mrad. The detector provides a measurement of the charge deposited in each of its  $2.5 \times 10^6$  strips. The position resolution is better than 20  $\mu\text{m}$  in the  $x$ - $y$  direction and about 0.8 mm in the direction along the beam line. The thickness of the SSD, including supports and services, corresponds to 2.2% of a radiation length. About 90% of the SSD area was active during data taking.
- The VZERO detector consists of two arrays of 33 scintillators each, which are placed around the beam pipe on either side of the interaction region. VZERO-A at  $z = 3.8$  m, covering the pseudorapidity range  $2.8 < \eta < 5.1$ , VZERO-C at  $z = -0.9$  m, covering the pseudorapidity range  $-8.0 < \eta < -1.7$ . The time resolution of this detector is better than 1 ns. Its response is recorded in a time window of  $\pm 25$  ns around the nominal beam crossing time. For events collected in this run, the arrival times of particles at the detector relative to this “time zero” is shown in Fig. 3. Note that in general several particles are registered on each scintillator, which falling out of the detector before the beam crossing have negative arrival times and are typically due to interactions taking place outside the central region of ATLAS.

More details about the ALICE experiment and its detector subsystems can be found in [2].

The trigger used to record the events for the present analysis is defined by requiring at least two hit chips in the SPD, in coincidence with the signals from the two beam-pickup counters, indicating the presence of two passing proton bunches. The efficiency of this trigger as well as all other corrections have been studied using two different Monte Carlo generators, PYTHIA 6.4.14 [32, 33] and TAT [34] and PROJET [16], for NNFF and NSD interactions. The trigger efficiencies for non-diffractive, single-diffractive, and double-diffractive events were evaluated separately, and found to be 98–99%, 48–50%, and 57–60% respectively. The ranges are determined by the two event generators. These event classes were combined for the corrections using the fractions measured by TAT [35]: non-diffractive 0.767  $\pm$  0.059, single-diffractive 0.153  $\pm$  0.023, double-diffractive 0.08  $\pm$  0.03. The resulting efficiencies were found to be 87–91% for the IN3, normalization and

Fig. 3 ALICE

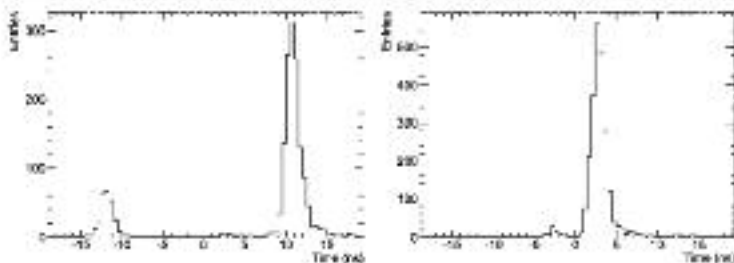


Fig. 3 Arrival time of particles in the ALICE detectors relative to the beam crossing time (time zero). A number of zero hits or hits in zero events are visible as secondary peaks in VZERO-A (left panel) and VZERO-C (right panel). This is because particles produced in each

detector interact from a pair of earlier events in one or the other of the two detectors. The majority of the signals have the correct arrival time associated to the beam crossing with the nominal vertex.

91–97% for the NSD normalization, again depending on the event generation used.

The results presented in the following sections are those obtained with PETHA. The difference between results constructed with PETHA and PHOET is used in the estimate of the systematic uncertainty.

4 Data analysis

The data sample used in the present analysis consists of 294 events recorded without magnetic field. The results presented here are based on the analysis of the SPD data. However, information from the SDD, SSD and VZERO was used to crosscheck the identification and removal of background events.

In the SPD analysis, the position of the interaction vertex is reconstructed [45] by correlating hits in the two adjacent layers to obtain tracks. The achieved resolution depends on the track multiplicity and for this specific vertex reconstruction is approximately 0.1–0.3 mm in the longitudinal direction and 0.3–0.5 mm in the transverse direction. For events with only one charged track, the vertex position is determined by matching the SPD tracks with the mean beam spot determined from the vertex position of other events in the sample. A vertex was reconstructed in 90% of the selected events. The distribution of the vertex position in the longitudinal direction (*z*-axis) is shown in Fig. 4. For events originating from the centre of the detector, the vertex reconstruction efficiency was estimated, using Monte Carlo simulations, to be 81% for INEL interactions and 92% for NSD collisions. These efficiencies decrease for larger  $|z|$ -values of the vertex in two-multiplicity events; therefore, only events with vertices within  $|z| < 10$  cm were used. This allows for an accurate charged-particle density measurement in the pseudorapidity range  $|\eta| = 1.6$  using both SPD layers.

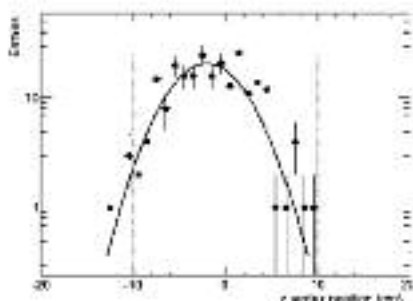


Fig. 4 Longitudinal vertex distribution from hit correlations in the two pixel layers of the ALICE inner tracking system. Vertical dashed lines indicate the beam spot size (10 cm), where the vertices for the present study are reconstructed. A Gaussian fit with an extension (sigma) of about 4 cm to the central part is also shown

Using the reconstructed vertex as the origin, we calculate the differences in azimuthal ( $\Delta\phi$ ), bending plane) and polar ( $\Delta\theta$ , see bending direction) angles of pairs of hits with one hit in each SPD layer. These tracksets [27] are selected by a cut on the ratio of the squares of  $\Delta\phi$  and  $\Delta\theta$ , each normalized to its estimated resolution (30 mrad and 25 mrad, respectively). When more than one hit in a layer matches a hit in the other layer, only the hit combination with the smallest angular difference is used. This occurs in only 2% of the matched hits.

The number of primary charged particles is estimated by counting the number of tracksets. This number was corrected for:

- trigger inefficiency;
- detection and reconstruction inefficiencies;

contamination by decay products of long-lived particles ( $K_S^0$ ,  $\Lambda$ , etc.) gamma conversions and secondary interactions.

The corrections are determined as a function of the  $x$ -position of the primary vertex, and on the pseudorapidity of the tracklets. For the analysed sample the average correction factor for tracklets is about 1.5.

The beam-gas and beam-halo background events were removed by a cut on the ratio between the number of tracklets and the total number of hits in the tracking system (SPD, SDD, and SSD). This ratio is smaller for background events (as measured in the previous file triggering on the bunch passage from one side) than for collisions [36]. In addition, the timing information from the VTX301 detector was used for background rejection by removing events with negative arrival time error (Fig. 3). The remaining background contamination was cross-checked by a visual scan of the whole event sample. In total 29 events (i.e. about 10%) were rejected as beam-induced background, which is consistent with the rate expected from previous files. The remaining background was estimated from the vertex distribution and found to be negligible. The contamination from coincidences with a cosmic muon was estimated to be one event in the full sample. Indeed, two cosmic events were identified by scanning, both without reconstructed vertex.

Particular attention has been paid to events having zero or one charged tracklet in the SPD acceptance. The event-finding efficiency for events with one charged particle in the acceptance is about 90%. The number of zero-track events has been estimated by Monte Carlo calculations. The total number of collisions used for the normalization was calculated from the number of events selected for the analysis, corrected for the vertex-reconstruction efficiency. In order to obtain the normalization for INEL and NSD events, we further corrected the number of selected events for the trigger efficiency for these two event classes. In addition, for NSD events, we subtracted the single-diffractive contribution. These corrections, as well as those for the vertex-finding efficiency, depend on the event charged-particle multiplicity, see Fig. 5. The dependence of the event-finding efficiency (combining event selection and vertex finding) on multiplicity was calculated for different interaction types using our detector simulation, and is about 98% for events with at least two charged particles. The averaged combined corrections for the vertex-reconstruction efficiency and the selection efficiency is 20% for INEL interactions and much smaller for NSD interactions, due to the cancellation of some contributions.

The various corrections mentioned above were calculated using the full GEANT 3 [39, 40] simulation of the ATLAS detector as included in the offline framework A3Flow. In order to estimate the systematic uncertainties, the above analysis was repeated by

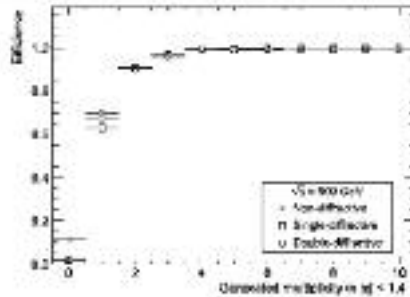
Fig. 7 (vs.  $T$ )

Fig. 8 Multiplicity dependence of the event-finding efficiency to select an event or maintain hits and to reconstruct the vertex in SPD, for non-diffractive (circles), single-diffractive (squares), and double-diffractive (triangles) events, based on PYTHIA events

- applying different cuts for the tracklet selection (varying the angle cut-off by  $\pm 5\%$ );
- varying by  $\pm 10\%$  the density of the material in the tracking system, thus changing the material budget;
- using the non-aligned geometry;
- varying by  $\pm 50\%$  the composition of the produced particle types with respect to the yields suggested by the event generators;
- varying the particle yield below 100 MeV/c by  $\pm 50\%$ ;
- evaluating the uncertainty in the normalization to INEL and NSD samples by varying the ratio of the non-diffractive, single-diffractive and double-diffractive cross sections according to their measured values and errors [34] and using two different models for diffractive kinematics (PYTHIA and PHOJET).

An additional source of systematic error comes from the limited statistics used so far to determine the efficiency of the SPD detector modules. In test beams, the SPD efficiency in active areas was measured to be higher than 99.9%. This was cross-checked in-situ with cosmic data, but only over a limited area and with limited statistics. At this stage, we have assigned a conservative value of 4% to this uncertainty. The triggering efficiency of the SPD was estimated from the data itself, using the trigger information recorded in the data stream for events with more than one tracklet, and found to be very close to 100%, with an error of about 2% due to the limited statistics.

These contributions to the systematic uncertainty on the charged-particle pseudorapidity density are summarized in Table 1. Our conclusion is that the total systematic uncertainty of the pseudorapidity density is less than 1.2% for INEL collisions and 17.1% for NSD collisions. The largest contribution comes from uncertainties in cross sections of diffractive processes and their kinematic distribution.

Tab. 1. Cont.

**Table 1** Contributions to systematic uncertainties on the estimation of the charged particle pseudorapidity density

| Contribution                        | [%]         |
|-------------------------------------|-------------|
| Track reconstruction                | 0.61        |
| Material budget                     | 0.61        |
| Misalignment                        | 0.52        |
| Particle composition                | 0.61        |
| Transverse momentum spectrum        | 0.95        |
| Classification of diffraction (IND) | 0.1         |
| Classification of diffraction (NSD) | ± 0.96      |
| Proton-antiproton dependence (M+D)  | 0.1         |
| Event plane dependence (MSD)        | 0.1         |
| Detector efficiency                 | 0.1         |
| RPD magnetic efficiency             | 0.6         |
| Background events                   | 0.61        |
| <b>Total (IND)</b>                  | <b>2.96</b> |
| <b>Total (NSD)</b>                  | <b>2.18</b> |

More details about this analysis, corrections, and the evaluation of the systematic uncertainties can be found in [41].

**5 Results**

Figure 6 shows the charged primary particle pseudorapidity density distributions obtained for IND and NSD interactions in the range  $|\eta| < 1.6$ . The pseudorapidity density obtained in the central region  $|\eta| < 0.5$  for IND interaction is  $3.10 \pm 0.13(\text{stat.}) \pm 0.22(\text{sys.})$  and for NSD interaction is  $3.51 \pm 0.15(\text{stat.}) \pm 0.25(\text{sys.})$ . Also shown in Fig. 6 are the previous measurements of proton-antiproton interactions from the UA5 experiment [3]. Our results obtained for proton-antiproton interactions are consistent with those for proton-antiproton interactions, as expected from the fact that the predicted difference ( $\delta$ ) = 0.29) is well below measurement uncertainties. The measurements at central pseudorapidity ( $|\eta| < 0.5$ ) are summarized in Table 2 together with model predictions obtained with QGS-M, PHO-

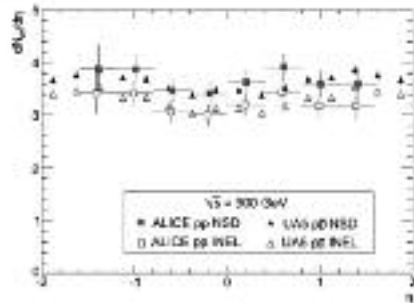


Fig. 6 Pseudorapidity dependence of  $dN_{ch}/d\eta$  for IND and NSD collisions. The ALICE measurements (square) are compared to UA5 data (triangles) [3]. The error shown are statistical only.

JET and three different PYTHIA tunes. PYTHIA 6.4.14, tune D6T and PHOJET yield respectively the lowest and highest charged particle densities. Therefore, these two have been used for the evaluation of our systematic errors. PYTHIA 6.4.20, tunes ATLAS CSC and Perugia-0, are candidates for use by the LHC experiments at higher LHC energies and are shown for comparison.

Figure 7 shows the centre-of-mass energy dependence of the pseudorapidity density in the central region ( $|\eta| < 0.5$ ). The data points are obtained in the  $|\eta| < 0.5$  range from this experiment and from references [5, 18, 19, 45–48], and are corrected for differences in pseudorapidity range where necessary, fitting the pseudorapidity distribution around  $\eta = 0$ . As noted above, there is good agreement between pp and p $\bar{p}$  data at the same energy. The dashed and solid lines (for IND and NSD interactions respectively) are obtained by fitting the density of charged particles in the central pseudorapidity region with a power law dependence on energy.

Using this parametrization, the extrapolation to the minimal LHC energy of  $\sqrt{s} = 14$  TeV yields  $dN_{ch}/d\eta = 3.3$  and  $dN_{ch}/d\eta = 3.5$  for IND and NSD interactions respectively.

**Table 2** Comparison of charged primary particle pseudorapidity density in central pseudorapidity  $|\eta| < 1.5$  for inelastic (IND) and non-diffractive (NSD) collisions measured by the ALICE detector in pp interactions and by UA5 in p $\bar{p}$  interactions [3] at a centre-of-mass energy of 900 GeV. For ALICE, the first error is statistical

| Interaction Model | ALICE [4]                | UA5 p $\bar{p}$ [3] | QGS-M [62] | PYTHIA [22, 75] |            |            | PHOJET [49] |
|-------------------|--------------------------|---------------------|------------|-----------------|------------|------------|-------------|
|                   |                          |                     |            | (199) [54]      | (200) [43] | (201) [44] |             |
| IND               | $3.10 \pm 0.12 \pm 0.22$ | $3.08 \pm 0.02$     | 2.98       | 2.53            | 2.99       | 2.46       | 3.14        |
| NSD               | $3.51 \pm 0.15 \pm 0.25$ | $3.40 \pm 0.07$     | 3.47       | 2.49            | 3.48       | 3.02       | 3.61        |

and the second is systematic; an overall error is given by 10%. The experimental data are also compared to the predictions for pp and p $\bar{p}$  from different models. For PYTHIA, the two versions are given in parentheses. The correspondence is as follows: (199) tune (199); ATLAS CSC tune (200); Perugia-0 tune (201).

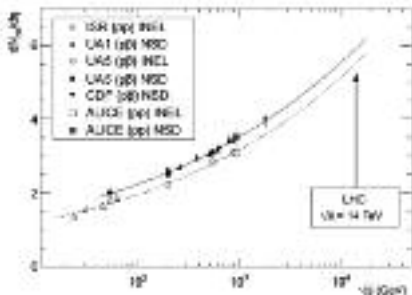


Fig. 7 Charged particle pseudorapidity density in the central rapidity region in proton-proton and proton-neutron interactions as a function of the center-of-mass energy. The UA5 and ALICE data points at 800 GeV are shaded differently to clearly distinguish the central and mid-rapidity data. The NIEL and NRD labels refer respectively to nuclear interaction data. The solid line represents a power-law dependence as in eq. (1)

6 Conclusion

Proton-proton collisions observed with the ALICE detector in the early phase of the LHC commissioning have been used to measure the pseudorapidity density of charged primary particles at  $\sqrt{s} = 900$  GeV. In the central pseudorapidity region ( $|\eta| < 0.5$ ), we obtain  $dN_{ch}/d\eta = 3.10 \pm 0.13(stat.) \pm 0.22(sys.)$  for all tracks and  $dN_{ch}/d\eta = 3.51 \pm 0.15(stat.) \pm 0.25(sys.)$  for non-emptied intermediate proton-proton interactions. The results are consistent with earlier measurements of primary charged-particle production in proton-nucleon interactions at the same energy. They are also compared with model calculations.

These results have been obtained with a small number of events during the early commissioning of the LHC. They demonstrate that the LHC and its experiments have finally entered the phase of physics exploration, within days of starting up the accelerator complex in November 2009.

**Acknowledgement** The ALICE collaboration would like to thank all the engineers and technicians for their invaluable contributions to the construction of the experiment. We would like to thank and congratulate the CERN accelerator team for the outstanding performance of the LHC complex in start-up, and for providing us with the collision conditions for the present production run.

The ALICE collaboration acknowledges the following funding agencies for their support in building and running the ALICE detector:

- Chinese Collaborating Institutions from Beijing and Shenyang, People's Republic of China;
- Conselho Nacional de Desenvolvimento Científico e Tecnológico (CNPq), Financiadora de Estudos e Projetos (FINEP), Fundação de Amparo à Pesquisa do Estado de São Paulo (FAPESP);
- National Natural Science Foundation of China (NSFC), the Chinese Ministry of Education (CMOE) and the Ministry of Science and Technology of China (MSTC).

- Ministry of Education and Youth of the Czech Republic, Czech National Science Research Council and the Caltech-CTSL collaboration;
- The European Research Council under the European Community's Seventh Framework Programme;
- Helsinki Institute of Physics and the Academy of Finland;
- French CNRS IN2P3, the "Region Pays de Loire - Région Auvergne", Région Auvergne and CNRS, France;
- German BMBWF and the Helmholtz Association;
- Hungarian OTKA and National Office for Research and Technology (OSZE);
- Department of Atomic Energy and Department of Science and Technology of the Government of India;
- Istituto Nazionale di Fisica Nucleare (INFN) of Italy;
- MEXT Directly and Specialized Financial Research Support – Accelerator for Nuclear Research (NHR);
- Korea Foundation for International Cooperation of Science and Technology (KICOS);
- CONACYT, DGAPA, México, ALFA, FC and the IFFIHT project (High Energy Physics Latin American Integration Network);
- Scientific user Facilities and Collaborative User Network (CUCAN) and the Polish-Lithuanian Organization for Nuclear Research (OZNA);
- STFC, UK;
- Research Council of Norway (NFR);
- Polish Ministry of Science and Higher Education;
- National Authority for Scientific Research-ANRS (actions de Recherche prioritaire Coopération Scientifique ANRS);
- National Agency of Science of the Ministry of Education and Science of Russian Federation, International Science and Technology Center, Russian Federal Agency of Atomic Energy, Russian Federal Agency for Science and Innovation and CERN (NTAS);
- Ministry of Education of Slovakia;
- CFMUT, IIT-A, Ministerio de Educación y Ciencia of Spain, Xerox de Galicia, Consellería de Educación, CEADEN, Colaboración Chile and IATA (International Atomic Energy Agency);
- Swedish Research Council (VR) and Knut and Alice Wallenberg Foundation (KAW);
- Chinese Ministry of Education and Science;
- United Kingdom Science and Technology Facilities Council (STFC);
- The United States Department of Energy, the United States National Science Foundation, the State of Texas, and the State of Ohio.

**Open Access** This article is distributed under the terms of the Creative Commons Attribution Non-commercial License which permits any non-commercial use, distribution, and reproduction in any medium, provided the original author(s) and source are credited.

References

1. J. Kwieciński, H. Nyska, J. Trnka, *J. Phys. G* **32**, 095001 (2006)
2. K. Andersson et al. (NIEL) Collaboration, *J. Instrum.* **3**, S09002 (2008)
3. G.J. Alford et al. (UA5 Collaboration), *Z. Phys. C* **35**, 1 (1988)
4. A.R. Kaidalov, *Phys. Lett. B* **116**, 495 (1983)
5. A.R. Kaidalov, K.A. Ter-Mikaelian, *Phys. Lett. B* **117**, 247 (1983)
6. A.R. Kaidalov, K.A. Ter-Mikaelian, *Sov. J. Nucl. Energy* **39**, 1545 (1984) (*Sov. J. Part. Nucl. Phys.* **39**, 979 (1984))
7. A.R. Kaidalov, K.A. Ter-Mikaelian, *Nucl. Phys. A* **40**, 71 (1986) (*Sov. J. Part. Nucl. Phys.* **40**, 152 (1986))
8. A. Capella et al., *Z. Phys. C* **3**, 323 (1980)
9. A. Capella, *J. Theor. High. Nucl. Phys. C* **10**, 369 (1981)
10. A. Capella, *J. Theor. High. Nucl. Phys. Lett.* **11**, 142, 496 (1982)

## Ref. Phys. J. C

11. A. Datta et al., *ScholarX*, 12-01-2019, <https://doi.org/10.21203/rs.3.rs-1000000/v1>, 2019
12. M.S. Amelin et al., *Phys. Lett. B*, **211** (1998) 450-454
13. M.S. Amelin et al., *Yad. Fiz.*, **57**, 512 (1994) (*Sov. J. Nucl. Phys.*, **57**, 527 (1994))
14. M.S. Amelin et al., *Yad. Fiz.*, **57**, 592 (1994) (*Sov. J. Nucl. Phys.*, **57**, 573 (1994))
15. E. Amaldi et al., *Phys. Rev. D*, **45**, 32 (1992)
16. R. Barsh et al., *Phys. Rev. D*, **32**, 1469 (1985)
17. G.L. Sushkov, S.K. Rind, *Phys. Rep.*, **7**, 46 (1970)
18. R. Appel et al., *NA55 Collaboration*, *Phys. Lett. B*, **112**, 169 (1992)
19. M. Ambrosio et al., *AT-Coll. Proc.*, **85**, 902 (1992)
20. C. Anders et al., *ALICE Internal Note ALICE-INT/2008-015* (2008)
21. T. Anders et al., *ALICE Collaboration*, *J. Phys. Conf. Ser.*, **114**, 022006 (2008)
22. ALICE Collaboration, *ALICE: OUTFITS, simulation, reconstruction and analysis framework*, <http://alice.root.cern.ch/Outfits>
23. T.M. Botteroth, *ALICE Collaboration*, in *Proceedings of COMP 2006, Mainz 2006*, Prague, *J. Phys. Conf. Ser.*, **114**, 022007 (2006)
24. ALICE Collaboration, *J. Phys. Conf. Ser.*, **1513** (2009)
25. ALICE Collaboration, *J. Phys. Conf. Ser.*, **1245** (2009)
26. M. D'Azavedo, *ALICE Collaboration*, *Nucl. Phys. A*, **830**, 81C (2009)
27. P. Fiala, *ALICE Collaboration*, *Nucl. Phys. A*, **830**, 820C (2009)
28. M. Sabel et al., *ALICE Collaboration*, *J. Instrum.*, **4**, 04002 (2009)
29. G. Sotiropoulos et al., *CERN preprint CERN 2004 043*, 2004
30. E. G. Ferrel et al., *ALICE Collaboration*, in *Proceedings of EPS-HEP 2005*, July 2005, Krakow, Preprint, arXiv:hep-ph/0507001
31. T. Kniehl et al., *ALICE Internal Note ALICE-INT-2009-003*, 2009
32. T. Sjostrand, *Comput. Phys. Commun.*, **82**, 74 (1994)
33. T. Sjostrand, G. Miu, S. Mrenca, *J. High Energy Phys.*, **2006**, 05 (2006)
34. M.O. Adams et al., *CBCLBC QCD Working Group*, <https://arxiv.org/abs/hep-ph/0212236>, 267-100 (2002)
35. R.L. Anderson et al., *PHS Collaboration*, *Z. Phys. C*, **33**, 125 (1986)
36. T. Anders et al., *ALICE Internal Note ALICE-INT-2006-018*, 2006
37. D. Anders et al., *ALICE Internal Note ALICE-INT-2009-021*, 2009
38. J.M. Casado-Ojeda et al., *ALICE Internal Note ALICE-INT-2009-022*, 2009
39. K. Binnig et al., *GLAS-11 User Book*, CERN, <http://cds.cern.ch/record/1101294>, 1995
40. K. Binnig et al., *GLAS-11 Program Library User's Guide*, 89913, CERN, <http://cds.cern.ch/record/1101294>, 1994
41. J.P. Chouinard, *Ph.D. thesis*, University of Montreal, GENEVA, 1990, CERN TH.5538, 1990-044
42. A.H. Kaidas, M.D. Pughorran, *Int. Phys. J. C*, *submitted*, <https://arxiv.org/abs/hep-ph/0204024> (2002)
43. A. Mincer, *GLAS Collaboration*, *GLAS Note NUC-CO04-THYS-2009-119*, 2009, <http://cds.cern.ch/record/1101294>
44. F. Skaala, *in: Hadron-Hadron Interactions*, *Proceedings, Perugia, Italy, 26-31 Oct. 2008*, [arxiv:hep-ph/0810207](http://arxiv.org/abs/hep-ph/0810207) (2008), Perugia-0 (2008) arXiv:hep-ph/0810207
45. S. Thomson et al., *Nucl. Phys. B*, **134**, 365 (1977)
46. C. Altarelli et al., *ALICE Collaboration*, *Nucl. Phys. B*, **835**, 261 (2009)
47. G.L. Sushkov et al., *ALICE Collaboration*, *Phys. Rep.*, **184**, 347 (1989)
48. F. Anders et al., *ALICE Collaboration*, *J. Phys. Conf. Ser.*, **1513**, 022001 (2009)